

# GSK-3 $\beta$ dysregulation contributes to parkinson's-like pathophysiology with associated region-specific phosphorylation and accumulation of tau and $\alpha$ -synuclein

JJ Credle<sup>1</sup>, JL George<sup>2</sup>, J Wills<sup>1</sup>, V Duka<sup>1</sup>, K Shah<sup>1</sup>, Y-C Lee<sup>3</sup>, O Rodriguez<sup>3</sup>, T Simkins<sup>4</sup>, M Winter<sup>1</sup>, D Moechars<sup>5</sup>, T Steckler<sup>5</sup>, J Goudreau<sup>4</sup>, DI Finkelstein<sup>2</sup> and A Sidhu\*,<sup>1</sup>

Aberrant posttranslational modifications (PTMs) of proteins, namely phosphorylation, induce abnormalities in the biological properties of recipient proteins, underlying neurological diseases including Parkinson's disease (PD). Genome-wide studies link genes encoding  $\alpha$ -synuclein ( $\alpha$ -Syn) and Tau as two of the most important in the genesis of PD. Although several kinases are known to phosphorylate  $\alpha$ -Syn and Tau, we focused our analysis on GSK-3 $\beta$  because of its accepted role in phosphorylating Tau and to increasing evidence supporting a strong biophysical relationship between  $\alpha$ -Syn and Tau in PD. Therefore, we investigated transgenic mice, which express a point mutant (S9A) of human GSK-3 $\beta$ . GSK-3 $\beta$ -S9A is capable of activation through endogenous natural signaling events, yet is unable to become inactivated through phosphorylation at serine-9. We used behavioral, biochemical, and *in vitro* analysis to assess the contributions of GSK-3 $\beta$  to both  $\alpha$ -Syn and Tau phosphorylation. Behavioral studies revealed progressive age-dependent impairment of motor function, accompanied by loss of tyrosine hydroxylase-positive (TH+ DA-neurons) neurons and dopamine production in the oldest age group. Magnetic resonance imaging revealed deterioration of the substantia nigra in aged mice, a characteristic feature of PD patients. At the molecular level, kinase-active p-GSK-3 $\beta$ -Y216 was seen at all ages throughout the brain, yet elevated levels of p- $\alpha$ -Syn-S129 and p-Tau (S396/404) were found to increase with age exclusively in TH+ DA-neurons of the midbrain. p-GSK-3 $\beta$ -Y216 colocalized with p-Tau and p- $\alpha$ -Syn-S129. *In vitro* kinase assays showed that recombinant human GSK-3 $\beta$  directly phosphorylated  $\alpha$ -Syn at a single site, Ser129, in addition to its known ability to phosphorylate Tau. Moreover,  $\alpha$ -Syn and Tau together cooperated with one another to increase the magnitude or rate of phosphorylation of the other by GSK-3 $\beta$ . Together, these data establish a novel upstream role for GSK-3 $\beta$  as one of several kinases associated with PTMs of key proteins known to be causal in PD.

Cell Death and Differentiation (2015) 22, 838–851; doi:10.1038/cdd.2014.179; published online 14 November 2014

After Alzheimer's disease (AD), Parkinson's disease (PD) is the second most prevalent neurodegenerative disease, characterized by selective loss of TH+ DA-neurons of substantia nigra (SN) with diminished production of dopamine (DA).<sup>1</sup> Genome-wide studies have identified *SNCA* and *MAPT*, genes encoding  $\alpha$ -synuclein ( $\alpha$ -Syn) and Tau, respectively, as having strong association to the genesis of PD.<sup>2–4</sup> Although the precise etiology of PD remains a mystery, *SNCA* amplifications and mutations directly link  $\alpha$ -Syn dysfunction to disease causation,<sup>5,6</sup> firmly establishing a role for  $\alpha$ -Syn in sporadic and familial PD, respectively.  $\alpha$ -Syn can be phosphorylated at several sites,<sup>7</sup> and the predominance of  $\alpha$ -Syn phosphorylated at serine 129 (S129) in Lewy bodies<sup>8</sup> suggests its phosphorylation status at S129 has an important pathological role. Various PD models have shown that phosphorylation at S129 enhanced  $\alpha$ -syn toxicity

resulting in accelerated motor abnormalities and loss of DA-neurons.<sup>9,10</sup>

Fewer studies have examined the role of Tau (or p-Tau) in PD, but interest in the field has grown since completion of several genome-wide association studies. p-Tau has been found to colocalize with  $\alpha$ -Syn in tissue from sporadic PD and dementia with Lewy bodies.<sup>11</sup> We<sup>12,13</sup> and others<sup>14,15</sup> have also identified p-Tau in different brain regions of PD, dementia with Lewy bodies, and AD. High levels of p-Tau have also been observed *in vivo* in several toxin<sup>16–18</sup> and transgenic  $\alpha$ -Syn models of PD,<sup>19,20</sup> suggesting that p-Tau may be an important common factor in the neurodegeneration of not only tauopathies but also of synucleinopathies, such as PD.<sup>21–24</sup> Most studies to date have focused on the formation and accumulation of Tau and p-Tau in idiopathic PD. Yet several studies have provided evidence that leucine-rich repeat kinase-2 (LRRK2),

<sup>1</sup>Department of Biochemistry, Georgetown University, Washington, D.C., USA; <sup>2</sup>Florey Institute of Neuroscience and Mental Health, University of Melbourne, Vic, 3010, Australia; <sup>3</sup>Department of Oncology, Georgetown University, Washington, D.C., USA; <sup>4</sup>Department of Neurology, Department of Pharmacology & Toxicology, Michigan State University, East Lansing, MI, USA and <sup>5</sup>Janssen Research & Development, a division of Janssen Pharmaceutica NV, Turnhoutseweg 30, Beerse, 2340, Belgium

\*Corresponding author: A Sidhu, Biochemistry Molecular Cell Biology, Georgetown University, NRB, W222, The Research Building, Room W222, 3970 Reservoir Road, NW, Washington, D.C. 20007, USA. Tel: +202 687 0282; E-mail: sidhua@georgetown.edu

**Abbreviations:** GSK-3 $\beta$ , glycogen synthase kinase-3 $\beta$ ; SN, Substantia nigra; TH, tyrosine hydroxylase; TG, transgenic; DA, dopamine; PLK, Polo-like kinase; GRK, G-coupled Receptor kinase; CK2, Casein kinase-2; PD, Parkinson's disease; AD, Alzheimer's disease; DLB, Dementia with Lewy Bodies; PTMs, post-translational modifications; dMRI, diffusion tensor magnetic resonance imaging

Received 05.5.14; revised 28.7.14; accepted 16.9.14; Edited by B Zhivotovsky; published online 14.11.14

a kinase, that when mutated is involved in familial forms of PD, can directly interact with, and activate GSK-3 $\beta$ , resulting in increased p-TAU formation.<sup>25,26</sup>

Among the kinases known to hyperphosphorylate Tau, glycogen synthase kinase-3 $\beta$  (GSK-3 $\beta$ ) may be the most important given its ability to phosphorylate Tau at the majority of its serine/threonine sites that cause associated toxicities in AD.<sup>27,28</sup> The importance of GSK-3 $\beta$  is illustrated in that it is embryonically lethal when knocked out in mice. Regulation of GSK-3 $\beta$  is tightly controlled through a series of direct and indirect measures. Direct regulation occurs through autophosphorylation at Tyr216,<sup>29,30</sup> resulting in a kinase-active form, p-GSK-3 $\beta$ -Y216, whereas phosphorylation at Ser9 results in a kinase-inactive state.<sup>31</sup> The activity of GSK-3 $\beta$  can also be controlled indirectly through binding to inhibitory complexes with other cytoplasmic proteins,<sup>32,33</sup> or through Wnt-mediated sequestration into multivesicular bodies<sup>34</sup> resulting in the physical separation of GSK-3 $\beta$  from its cytoplasmic targets. Control of GSK-3 $\beta$  in the normal state is therefore tightly regulated, with its dysregulation and ensuing aberrant phosphorylation of targets being a common occurrence in many diverse diseases. Several studies have shown that GSK-3 $\beta$  is an important mediator in the injury and repair processes of neurons during cross-talk between DA-neurons and reactive astrocytes.<sup>35,36</sup> These studies showed that astrocyte-derived Wnt1 was capable of blocking GSK-3 $\beta$  activation, allowing the nuclear accumulation of  $\beta$ -catenin and subsequent gene expression of  $\beta$ -catenin-dependent targets essential for neuron survival and repair during chemical or metabolic insults. The importance of regulating the active/inactive states of GSK-3 $\beta$  in regard to neuronal stability is further supported through the analysis of conditional (Tet-inducible) transgenic mice expressing a dominant-negative GSK-3 $\beta$ -K85R mutant or expressing the GSK-3 $\beta$ -S9A mutant.<sup>37,38</sup> In these studies, post-natal Tet-regulated expression of either GSK-3 $\beta$ -K85R or GSK-3 $\beta$ -S9A led to neurodegeneration in the cortex, striatum, and hippocampus. What separates our TG PD model from the tet-inducible GSK-3 $\beta$  models is the spatial patterns of transgene expression, which is influenced by the choice of promoters. The Tet-inducible GSK-3 $\beta$  models are expressed using a CAMKII promoter with our human(h) GSK-3 $\beta$ -S9A transgene being expressed under the Thy-1 promoter. CAMKII-driven expression is limited to neurons originating from the forebrain with Thy-1 promoter-driven expression restricted to neurons in all or most brain regions.<sup>39,40</sup> Although promoter choice effecting tissue expression ultimately decides which regions show degeneration, the important message is that both inactive and hyperactive states of GSK-3 $\beta$  reduce neuronal viability.

In our past studies in various *in vitro* and *in vivo* models of PD and in postmortem PD tissues, we have consistently observed a positive correlation between increased  $\alpha$ -Syn and p-Tau levels with increased GSK-3 $\beta$ -Y216 (the kinase-active form of GSK-3 $\beta$ ).<sup>12,13,16,19,20</sup> In *in vitro* studies of MPTP-treated SH-SY5Y cells, blockade of GSK-3 $\beta$  with lithium, or with the highly selective non-ATP competitive inhibitor, TDZD-8, prevented the induction of p-GSK-3 $\beta$ -Y216, abolished p-Tau formation, and reversed the accumulation and aggregation of both p-Tau and  $\alpha$ -Syn, averting cell death.<sup>16</sup> Other studies using Rotenone or MPTP/MPP+ in chemical PD

models, have shown similar results of decreased neuronal viability during treatments accompanied by dose- and time-dependent increases in GSK-3 $\beta$  activation, with decreased cytotoxicity detected when GSK-3 $\beta$  was inhibited or knocked-down through the use of GSK-3 $\beta$ -specific small molecule inhibitors or through RNAi.<sup>41,42</sup> This suggested to us that p-GSK-3 $\beta$ -Y216 may have a contributory role in the pathogenesis of PD. Using a mouse model overexpressing hGSK-3 $\beta$ -S9A under the Thy-1 promoter together with *in vitro* kinase assays allowed us to discern the role GSK-3 $\beta$  has in the development of PD-like pathology.<sup>43</sup> Analysis of our hGSK-3 $\beta$ -S9A mouse model showed here for the first time that upon aging, these mice develop the cardinal features of parkinsonism, manifested as impaired motor behavior, with associated loss of TH+ neurons, reduced DA production, and shrinkage of SN. *In vitro* kinase assays confirmed that hGSK-3 $\beta$  was capable of phosphorylating  $\alpha$ -Syn on Serine 129 together with the known ability to phosphorylate Tau. Remarkably, both  $\alpha$ -Syn and Tau influenced the rate and magnitude of phosphorylation of the other by GSK-3 $\beta$  indicating that an intimate physical relationship exist between the trio of PD related proteins. Together, these data shown indicate the importance of GSK-3 $\beta$  activation, in the behavioral and physiological development of PD like pathology in a new mouse model.

## Results

**Progressive age-dependent motor deficits are associated with pathological declines in the SN of the hGSK-3 $\beta$ -S9A PD mouse model.** To directly test for a role of GSK-3 $\beta$  in PD *in vivo*, we conducted biochemical analysis at 4–6, 9, and 15 months of age, with behavioral analysis performed at 4–6, 9, 12, and 15 months of age on hGSK-3 $\beta$ -S9A transgenic mice. Rotarod testing revealed significant and progressive performance deterioration in TG mice at 12 and 15 months compared with age-matched wild-type (WT) controls and mice at younger ages (Figure 1a). TG mice also performed poorly in wire-hang tests, decreasing to 50% of controls (Figure 1b). TG mice showed progressively diminished age-dependent balance and co-ordination in pole tests that became significant at 12 and 15 months (Figure 1c). In gait tests (Figure 1d), the length of stride was progressively reduced, with ~50% decrease observed in 15-month-old TG mice. With declines in all behavioral tests becoming significant at 15 months, we decided to apply biochemical and physiological analysis on this particular age group of TG and WT mice. Such cumulative loss of motor function was accompanied by a significant loss of ~20% of tyrosine hydroxylase-positive (TH+) neurons in SN of 15-month-old TG mice (Figures 1e and 1f), as assessed by unbiased stereological counting, without any changes in non-TH+ neurons (Figure 1f), indicating a selective loss of DA-neurons. Although selective loss of DA-neurons is commonly observed in toxin-based models of PD, it is only rarely seen in genetic animal models of PD. For a comprehensive review and comparison of behavioral and physiological traits seen in transgenic PD mouse models, please see Chesslet and Richter.<sup>44</sup>

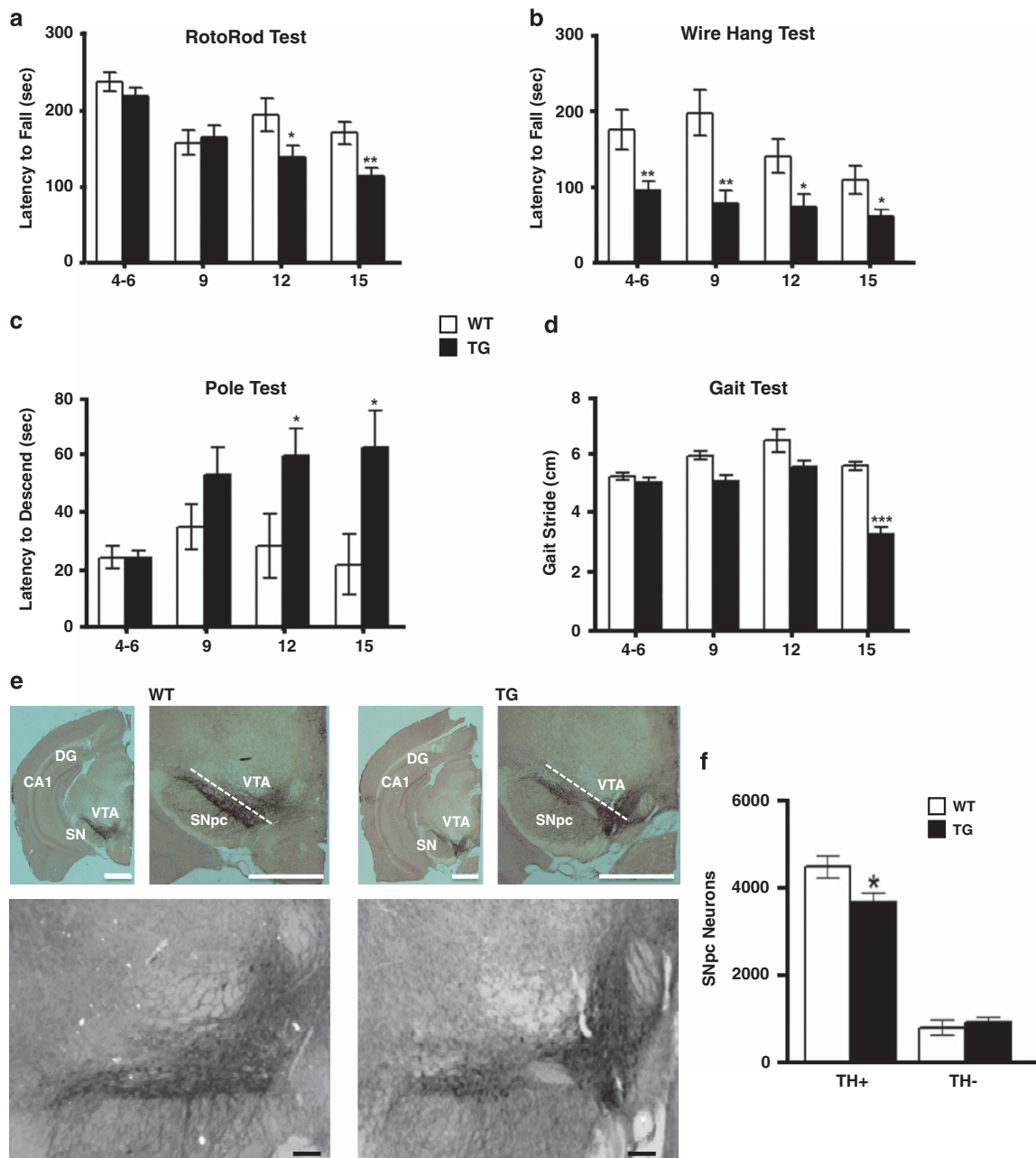


**Figure 1** Behavioral and histochemical analyses of hGSK-3 $\beta$ -S9A overexpressing and WT mice. TG and WT mice aged 4–6 (TG N=15; WT N=18), 9 (TG N=13; WT N=18), 12 (TG N=12; WT N=10), and 15 months (TG N=10; WT N=10) were used to measure motor impairment and motor co-ordination. (a) Rotarod tests, (b) Wire-hang tests, (c) pole tests (d) gait tests. Comparisons between age-matched WT and TG mice, as well as between TG mice of different ages were made using Welch's t test or one-way ANOVA, and significance was measured as \*P<0.05 or \*\*P<0.01 or \*\*\*P<0.001. (e) Unbiased stereological counts of TH-stained SN were conducted as described before,<sup>38</sup> using four mice at 15 months of age and both TH+ and TH- neurons were counted. (f) Scale bars on the upper panels represent 750  $\mu$ m, whereas on lower panels, the scale bars are 100  $\mu$ m. Dashed line denotes SN and VTA border with dentate gyrus (DG) and hippocampus (CA1) regions labeled for comparison. See also Supplementary Figure S1A and D

To assess changes in the anatomical structure of the TG mouse, we conducted magnetic resonance imaging (MRI) using the diffusion tensor imaging modality technique. Diffusion MRI (Supplementary Figures S1A and C) showed significant reduction of SN volume (Supplementary Figure S1B) in 15, but not in 4-month-old mice (Supplementary Figure S1C). Reduced volume of the SN has also been reported by MRI

analysis of PD patients correlating with motor decline.<sup>45,46</sup> In concordance with earlier reports,<sup>43</sup> these TG mice at 4 months also had significantly lower total brain volume (Supplementary Figure S1C) compared with age-matched WT mice, but at 15 months, brain volume had recovered and was equivalent between TG and WT mice. Loss of DA-neurons and diminished SN volume was also accompanied by a substantial

decrease of ~60% in levels of DA produced in midbrain of 15-month-old TG mice (Supplementary Figure S1D). A 60% decrease in striatal DA levels accompanied by a 20% decrease in TH+ DA-neurons of the SN pars compacta (SNpc) is consistent with previous studies analyzing  $\alpha$ -Syn TG PD models together with postmortem analysis of PD tissue.<sup>47–49</sup> In these studies, striatal DA was reduced 70–80% because of the early symptomatic degeneration of synaptic striatal innervations from TH+ cells of the SNpc. Yet, such significant loss of striatal DA co-occurred with less than 30% loss of the nigral DA cell bodies in the SNpc.

**Region and age-specific analysis of GSK-3 $\beta$  phosphorylation states in the hGSK-3 $\beta$ -S9A PD mouse model.** In order to assess how the kinase activity of GSK-3 $\beta$  is developmentally regulated in various brain regions, levels of GSK-3 $\beta$  and its differentially phosphorylated forms, p-GSK-3 $\beta$ -S9 (kinase-inactive) and p-GSK-3 $\beta$ -Y216 (kinase-active), were examined in three different brain regions of 4–6, 9, and 15-month-old mice: midbrain (Figures 2a and b), striatum (Figures 2c and d), and frontal cortex (Figures 2e and f). Significantly increased levels of p-GSK-3 $\beta$ -Y216 were found at most ages in midbrain, striatum, and frontal cortex. Levels of p-GSK-3 $\beta$ -S9 were significantly increased only in the midbrain of 15-month-old TG mice, and were unchanged at all other ages and brain regions, relative to WT. It should be noted that this reflects the phosphorylation of endogenous GSK-3 $\beta$ , as the transgene is incapable of being phosphorylated at serine 9. Increased levels of p-GSK-3 $\beta$ -S9 seen in the midbrain may represent a compensatory mechanism in which the cell is trying to mitigate the cytotoxic consequences of having increased levels of p-GSK-3 $\beta$ -Y216. Total GSK-3 $\beta$  levels were significantly increased at most ages and across most brain regions. Expression of p-GSK-3 $\beta$ -Y216 was confined to neuronal cells as evidenced by its colocalization with DARPP-32-positive neurons in the cortex and striatum of TG animals (Supplementary Figures S3E,F). p-GSK-3 $\beta$ -Y216-positive staining did not colocalize with GFAP-positive cells in the midbrain of TG animals, demonstrating that expression of the transgene was confined to neuronal populations and not expressed in non-neuronal glial cells (Supplementary Figure S3G).

Additional analysis of GSK-3 $\beta$  expression and p-GSK-3 $\beta$ -Y216 formation was confirmed by immunohistochemical (IHC) studies conducted on midbrain sections of 15-month-old WT and TG mice showing that both the phosphorylated and unphosphorylated forms were localized to TH+ DA-neurons (Figures 2g, h). Interestingly, IHC of paraffin-embedded PD human SN also demonstrated increased levels of p-GSK-3 $\beta$ -Y216 (Figure 2i, upper panel) which were accumulated in LBs and in neurites, and which were absent in non-diseased age-matched controls. As expected, elevated levels of  $\alpha$ -Syn immunostaining were also seen in LBs of PD SN neurons (Figure 2i, lower panel). Although we have analyzed total GSK-3 $\beta$  and p-GSK-3 $\beta$ -S9 in brains of PD patients by immunoblotting,<sup>12,13</sup> this is the first study to provide direct immunopositive evidence of increased p-GSK-3 $\beta$ -Y216 expression in DA-neurons of SN from PD patients.

**Age-specific hyperphosphorylation of tau at multiple sites is restricted to neurons in the striatum and midbrain of the GSK-3 $\beta$ -S9A PD mouse model.** In postmortem PD striatum, we have recently examined 20 different epitopes of p-Tau and found hyperphosphorylation to occur at 10 sites.<sup>12</sup> We, therefore, examined the pattern of Tau hyperphosphorylation by immunoblotting at these 10 epitopes in midbrain (Figures 3a and b), striatum (Figures 3c and d), and frontal cortex (Figures 3e and f) of 15-month-old TG and control mice. In midbrain, significant hyperphosphorylation was seen at 8 of the 10 epitopes examined (T205, T212, S235, S262, S356, S396/404, S409, and S422). When p-Tau sites were probed in striatum, we found a somewhat different profile, where just 5 of the 10 sites were hyperphosphorylated (S202, S235, S356, S396/404, and S409). Interestingly, we found significant decreases in phosphorylation at T212, S262, and S422. When frontal cortex was examined, to our surprise, we found no changes at any of the 10 p-Tau epitopes examined (Figure 3e), despite observing large increases in p-GSK-3 $\beta$ -Y216 in this region (Figures 2e and f). IHC (Figure 3g) confirmed the presence of p-Tau (S396/404 Tau) in DA-neurons of the midbrain from 15-month-old animals, colocalizing with TH. Interestingly, at younger ages, elevated levels of p-Tau were seen only in the striatum of 9-month-old TG mice, but were not found in other brain regions or at 4–6 months of age (Supplementary Figures S3A and D). In human PD SN, p-Tau (S396/404 Tau) immunostaining was observed as aggregates, and were also present in neurites (Figure 3h).

**Age-specific accumulation of p- $\alpha$ -Syn-S129 in TH+ neurons of the midbrain.**  $\alpha$ -Syn and TH levels were also assessed in the midbrain, striatum, and frontal cortex of 15-month-old mice (Figures 4a–c). Increased levels of  $\alpha$ -Syn expression were seen in the midbrain, striatum, and frontal cortex of 15-month-old TG mice. At younger ages (Supplementary Figures S3A and D), elevated levels of  $\alpha$ -Syn were seen only in the striatum of 9-month-old mice, but not in the midbrain or frontal cortex. Interestingly, TH expression levels were significantly decreased (by ~40%) only in the midbrain of 15-month-old TG mice (Figures 4a and b), correlating with the loss of TH+ neurons seen by nonbiased stereological counting (Figures 1e and f). Such loss of TH immunoreactivity in the midbrain was not observed in other brain areas or at younger ages (Supplementary Figures S3A and D), and instead, at 4–6 and 9 months, TH levels in midbrain of TG mice were slightly increased with time. Increased levels of TH seen in asymptomatic 4–6 and 9-month-old TG mice are consistent with the theory of the plasticity of the nigral-striatal pathway in PD.<sup>50,51</sup>

Several lines of evidence indicate that phosphorylation of  $\alpha$ -Syn at S129 is a highly toxic event, promoting its mis-folding, aggregation, and accumulation, and that its presence causes PD-associated degeneration of DA-neurons.<sup>7–10</sup> The ability of p-GSK-3 $\beta$ -Y216 to phosphorylate  $\alpha$ -Syn is not known. However, as both p-GSK-3 $\beta$ -Y216 and  $\alpha$ -Syn showed increased expression in DA-neurons, and that these DA-neurons showed deterioration at the 15 months of age, it seemed logical to question whether  $\alpha$ -Syn could be a potential substrate of phosphorylation by p-GSK-3 $\beta$ -Y216.

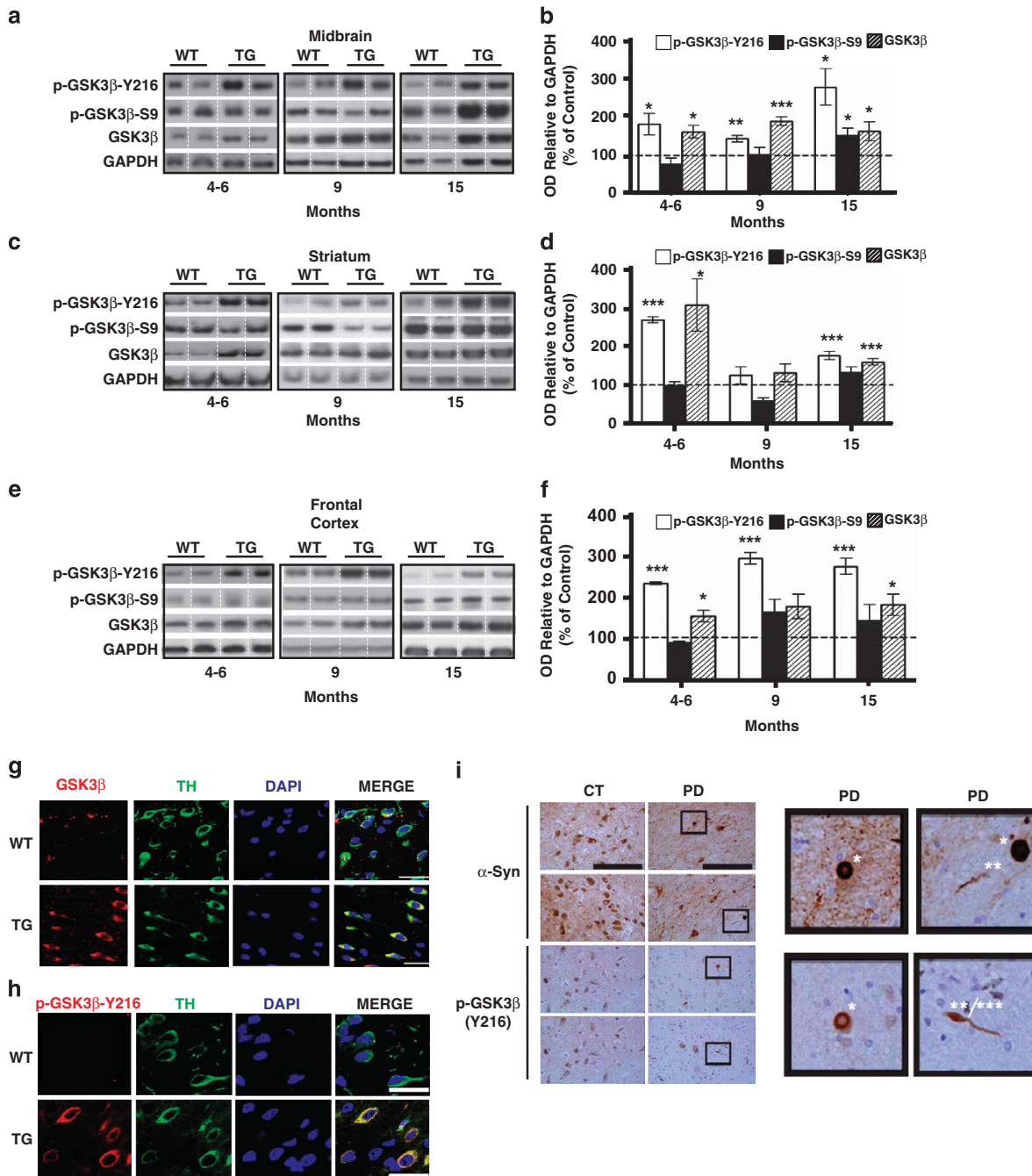


**Figure 2** Phospho-isoforms of GSK-3 $\beta$  in different brain regions and at different ages. Midbrain, striatum, and frontal cortex were analyzed from TG and WT mice at 4–6 ( $N=6$  each for TG and WT), 9 ( $N=8$  each for TG and WT) and 15 months ( $N=8$  each for TG and WT) for the differentially phosphorylated isoforms of GSK-3 $\beta$ . (a, b) midbrain (MB). (c, d) striatum (STR). (e, f) frontal cortex (FC). Immunohistochemical analyses from 15-month-old WT or TG mice ( $N=4$  each) were conducted using 10-micron-thick sections. (g) GSK-3 $\beta$ /TH. (h) p-GSK-3 $\beta$ -Y216/TH. IHC of paraffin-embedded human non-diseased (control, CT) and PD postmortem SN showing  $\alpha$ -Syn or p-GSK-3 $\beta$ -Y216 expression. (i) All WT values of proteins in western blots were normalized to GAPDH and set at 100%, denoted by the dashed line, and showed <10% variation at each data point. TG values were expressed relative to the WT control from within the same age group, after normalization to GAPDH, used as the loading control. Comparisons between age-matched WT and TG mice were made using Welch's *t* test or one-way ANOVA, and significance was measured as \* $P<0.05$  or \*\* $P<0.01$  or \*\*\* $P<0.001$ . Scale bar denotes 10  $\mu$ m in (g,h). In (i), scale bars correspond to 200  $\mu$ m and \* shows Lewy bodies, \*\* neurites, and \*\*\* aggregates. See also Supplementary Table S2

Immunoblotting analysis (Figures 4d and e) showed elevated levels of p- $\alpha$ -Syn-S129 in midbrain and striatum (200% and 80%, respectively) of 15-month-old TG, yet was absent in the frontal cortex. Moreover, p- $\alpha$ -Syn-S129 was not seen at 4–6 or 9 months of age, indicating that the presence of this

potentially toxic form paralleled the development of motor abnormalities and other PD-like pathology apparent at 15 months. IHC showed robust expression of p-Syn-S129 in TH+ neurons of the midbrain in 15-month-old TG, but not in WT mice (Figure 4f). Furthermore, p-GSK-3 $\beta$ -Y216 and

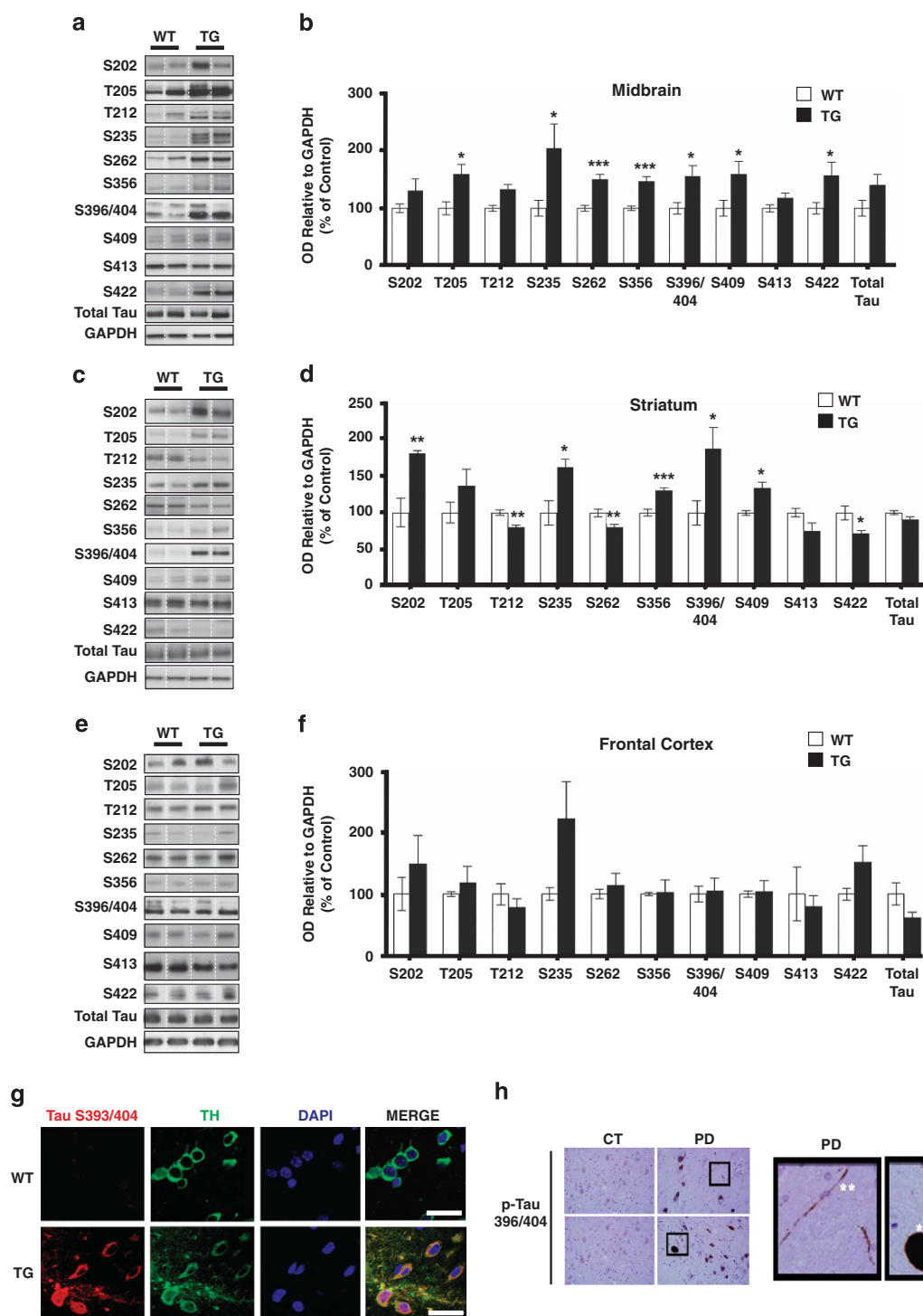


**Figure 3** Regional and age-specific accumulation of differentially phosphorylated Tau epitopes in WT and TG mice. The midbrain (**a**, **b**), striatum (**c**, **d**), and frontal cortex (**e**, **f**) from TG and WT mice ( $N=8$  each) at 15 months of age were analyzed by immunoblotting for various tau-phosphorylated epitopes. (**g**) IHC of TG and WT mouse brain. (**h**) IHC of paraffin-embedded human non-diseased (control) and PD postmortem SN for pTau(Ser396/Ser404). Comparisons between age-matched WT and TG mice were made using Welch's *t* test or one-way ANOVA, and significance was measured as \* $P<0.05$  or \*\* $P<0.01$  or \*\*\* $P<0.001$ . Scale bar on the IHC in (**g**) denotes 10  $\mu$ m. In (**h**), scale bars correspond to 200  $\mu$ m and \* shows Lewy bodies, \*\* neurites, and \*\*\* aggregates. See also Supplementary Figure S2B, S3A and G, and Supplementary Table S2

p- $\alpha$ -Syn-S129 colocalized with one another in midbrain neurons of TG mice, strongly suggestive of their involvement in the selective death of this specific subgroup of neurons (Figure 4g).

**In vitro kinase assays reveal that GSK-3 $\beta$  phosphorylates  $\alpha$ -Syn at a single site, serine-129.** Because the effect of p-GSK-3 $\beta$ -Y216 on p- $\alpha$ -Syn-S129 may have been indirect, we directly examined the ability of this kinase to

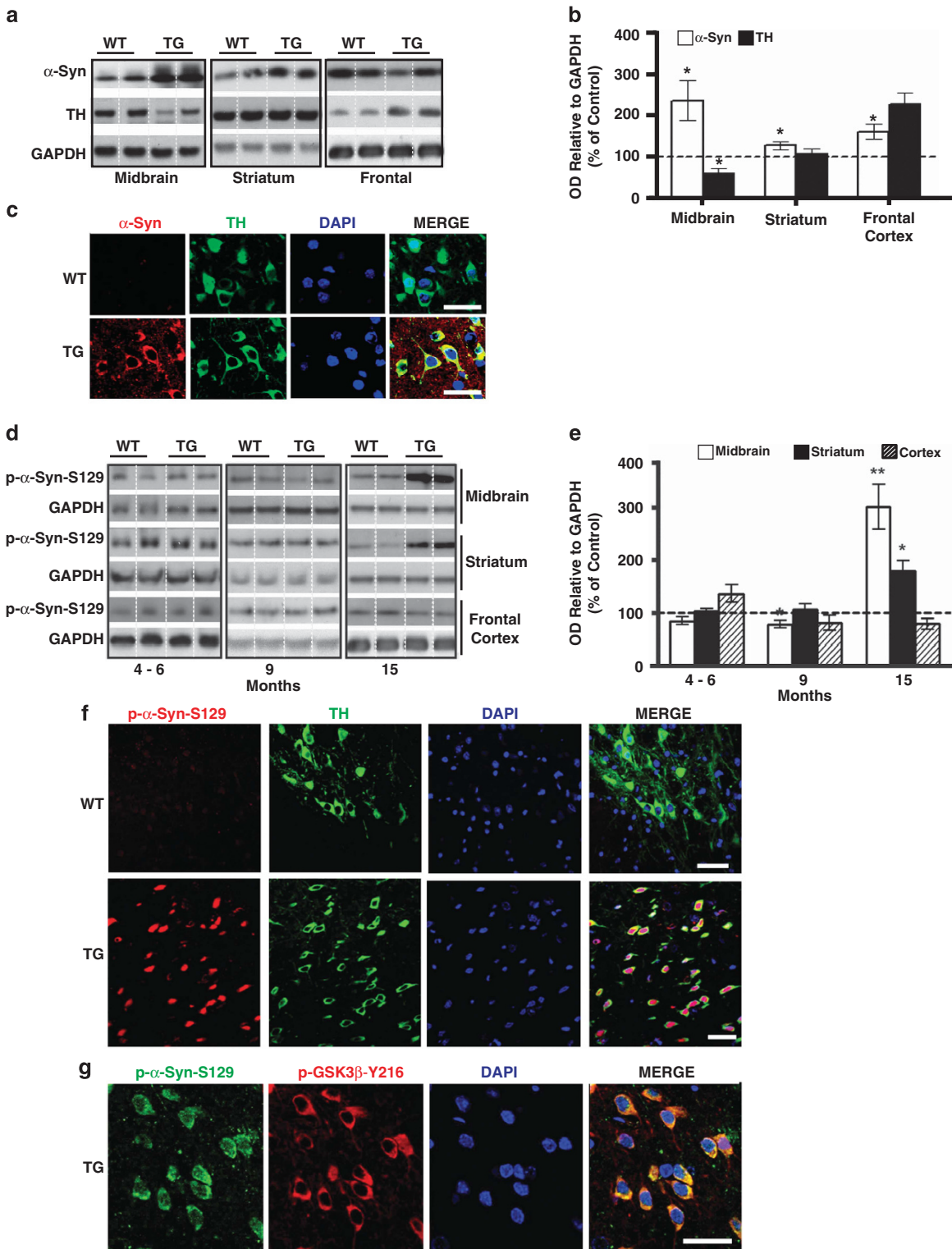


**Figure 4** Regional and age-specific accumulation of phosphorylated  $\alpha$ -Syn at S129 in WT and TG mice. (a,b)  $\alpha$ -Syn and TH levels were examined in midbrain (MB), striata (STR), and frontal cortex (FC) tissue from 15-month-old WT and TG mice ( $N=5$ ). (c) IHC comparison of  $\alpha$ -Syn immunoreactivity in TH+ neurons in age-matched 15-month-old WT and TG mice. (d,e) p- $\alpha$ -Syn-S129 levels were examined in midbrain (MB), striata (STR), and frontal cortex (FC) tissue from 4–6, 9, and 15-month-old WT and TG mice ( $N=5$ ). (f) IHC comparison of p- $\alpha$ -Syn-S129 immunoreactivity in TH+ neurons in age-matched 15-month-old WT and TG mice. (g) Co-localization of p- $\alpha$ -Syn-S129 immunoreactivity with p-GSK3 $\beta$ -Y216 in the SN of age-matched 15-month-old WT and TG mice. Comparisons between age-matched WT and TG mice were made using Welch's t test or one-way ANOVA, and significance was measured as \* $P<0.05$  or \*\* $P<0.01$  or \*\*\* $P<0.001$ . Scale bar on the IHC in (g) denotes 10  $\mu$ m. See also Supplementary Figures S2A, S3A, and G, and Supplementary Figures S5A and B

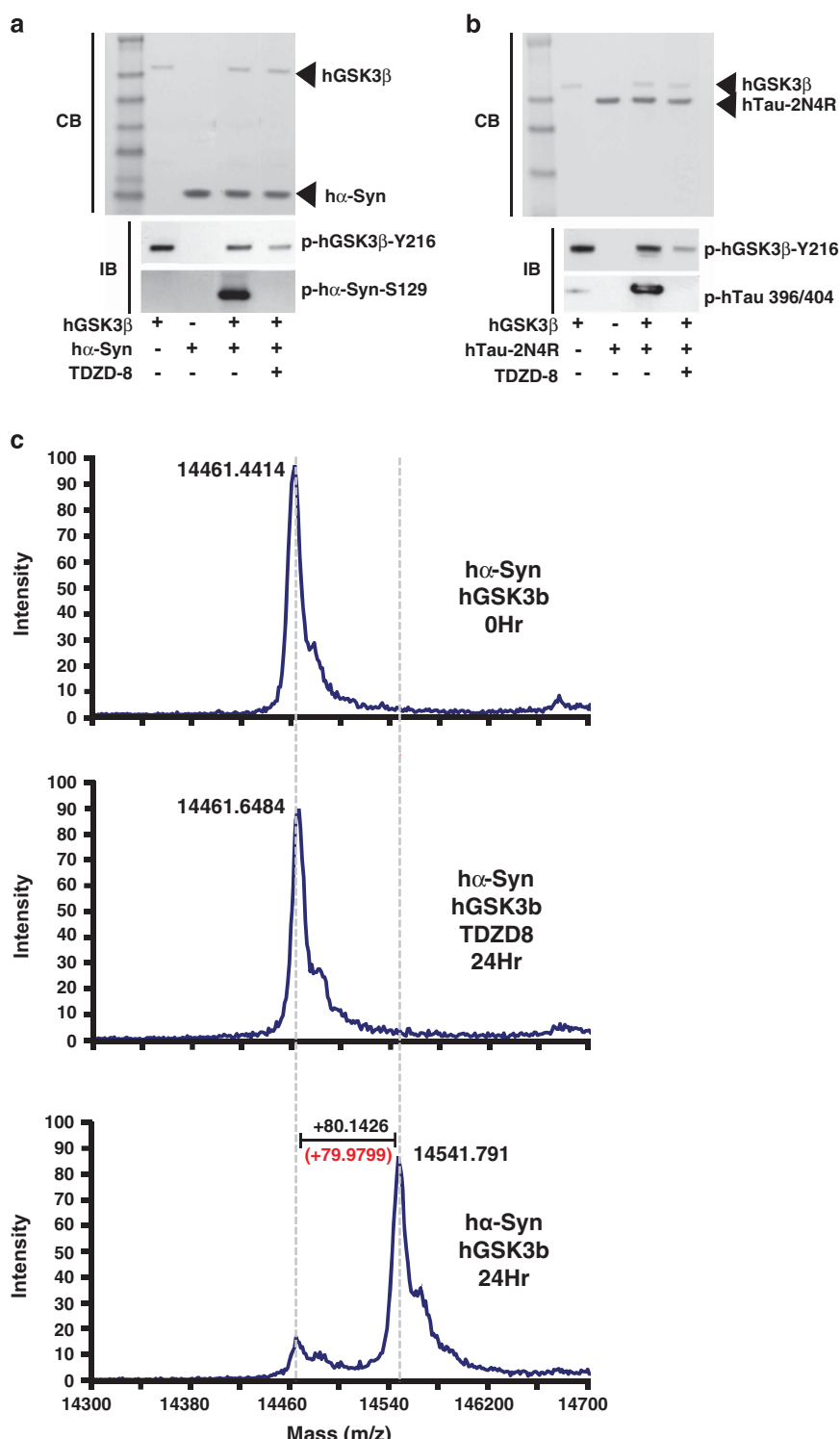


**Figure 5** *In vivo* phosphorylation of  $\alpha$ -Syn and Tau-2N4R by GSK-3 $\beta$ . Recombinant human proteins ( $\alpha$ -Syn, hGSK-3 $\beta$ , and hTau-2N4R) were purified as described in Methods (Supplementary Information), and purity was confirmed by coomassie blue (CB) staining of gels. For the *in vitro* reactions (a, b), 74.21 ng (3.34 nM) of recombinant hGSK-3 $\beta$  was incubated at room temperature for 24 h with either 1.45  $\mu$ g (3.34  $\mu$ M) of  $\alpha$ -Syn or 4.59  $\mu$ g (3.34  $\mu$ M) hTau-2N4R, in the absence or presence of 1  $\mu$ M of the hGSK-3 $\beta$  inhibitor, TDZD-8.<sup>16</sup> Proteins were analyzed by CB staining to determine purity and by immunoblots to determine phosphorylated epitopes. MS analysis of *in vitro* kinase reactions (c)  $\alpha$ -Syn and hGSK-3 $\beta$  0-h reaction (upper panel).  $\alpha$ -Syn and hGSK-3 $\beta$  with TDZD8 24-h reaction (middle panel).  $\alpha$ -Syn and hGSK-3 $\beta$  24-h reaction (lower panel). Calculated mass difference (black) comparing 0-h reaction (control) to 24-h reaction (lower panel) with theoretical mass difference of single phosphorylation (red) shown for reference. Each reaction was analyzed by western blots from three separate and independent studies

phosphorylate  $\alpha$ -Syn *in vitro*, using purified recombinant human proteins, whose purity (>95%) was confirmed by coomassie blue staining (Figure 5a). Endpoint analysis of GSK-3 $\beta$ / $\alpha$ -Syn kinase reactions showed that GSK-3 $\beta$  was converted to p-GSK-3 $\beta$ -Y216, with attendant  $\alpha$ -Syn phosphorylation at S129 (Figure 5a, lanes 2 and 4). If GSK-3 $\beta$  was omitted from the reaction mixture or if the reaction was co-incubated with 1  $\mu$ M TDZD-8, a highly specific and selective inhibitor of GSK-3 $\beta$ ,<sup>52</sup> the conversion of GSK-3 $\beta$  to p-GSK-3 $\beta$ -Y216 was reduced, with complete inhibition of  $\alpha$ -Syn phosphorylation at S129 (Figure 5a, lanes 3 and 5). Phosphorylation of Tau-2N4R, a known substrate of GSK-3 $\beta$  was also analyzed in *in vitro* kinase assays under equivalent conditions as had been performed when testing  $\alpha$ -Syn. Under these conditions, phosphorylation of Tau at S396/404 was appropriately observed (Figure 5b, lane 4). Omission of GSK-3 $\beta$  or addition of TDZD-8 again reduced the autophosphorylation of GSK-3 $\beta$  to p-GSK-3 $\beta$ -Y216, while simultaneously suppressing the ability of p-GSK-3 $\beta$ -Y216 to phosphorylate Tau.

Mass spectroscopy was performed to verify and assess the extent of phosphorylation of  $\alpha$ -Syn in 0 h and 24 h *in vitro* kinase reactions containing recombinant  $\alpha$ -Syn and GSK-3 $\beta$  +/- TDZD8. Zero hour kinase reactions (upper panel) or 24-h kinase reactions (middle panel) containing TDZD8 showed no change in the mass of  $\alpha$ -Syn (Figure 5c).  $\alpha$ -Syn was readily phosphorylated by p-GSK-3 $\beta$ -Y216 as shown by a change in mass from 14461.4414 to 14541.791 in the 24-h kinase reaction (Figure 5c, lower panel). The observed difference in mass of +80.1426 is very close to the theoretical change of 79.9799 associated with a single phosphorylation event on  $\alpha$ -Syn (Figure 5c, lower panel). These results suggest that GSK-3 $\beta$  phosphorylates  $\alpha$ -Syn at a single site, namely S129.

**$\alpha$ -Syn and tau influence GSK-3 $\beta$  by increasing the magnitude and rate of phosphorylation.** Time course studies (0–24 h), in the absence or presence of trace amounts of  $\alpha$ -Syn or Tau, were performed to examine the contribution of each protein on p-GSK-3 $\beta$ -Y216-mediated phosphorylation of the other protein. In other words, we wanted to determine whether the presence of Tau accelerated the rate of p- $\alpha$ -Syn-S129 formation and/or whether it increased the amount of p- $\alpha$ -Syn-S129 formed and *vice versa* using previously established kinase assay conditions. In the absence of Tau, the  $t_{1/2}$  of p- $\alpha$ -Syn-S129 formation was >480 min (Figures 6a and b). In the presence of trace amounts of Tau, however, the rate at which p- $\alpha$ -Syn-S129 formed was greatly accelerated, with its  $t_{1/2}$  now reduced to 60 min (Figure 6c). However, Tau did not alter the overall amount of p- $\alpha$ -Syn-S129 formed, and after 24 h, an equivalent amount of p- $\alpha$ -Syn-S129 was seen, regardless of the presence or absence of Tau (Figure 6b). Such acceleration of p- $\alpha$ -Syn-S129 by Tau was not due to increases in the rate or

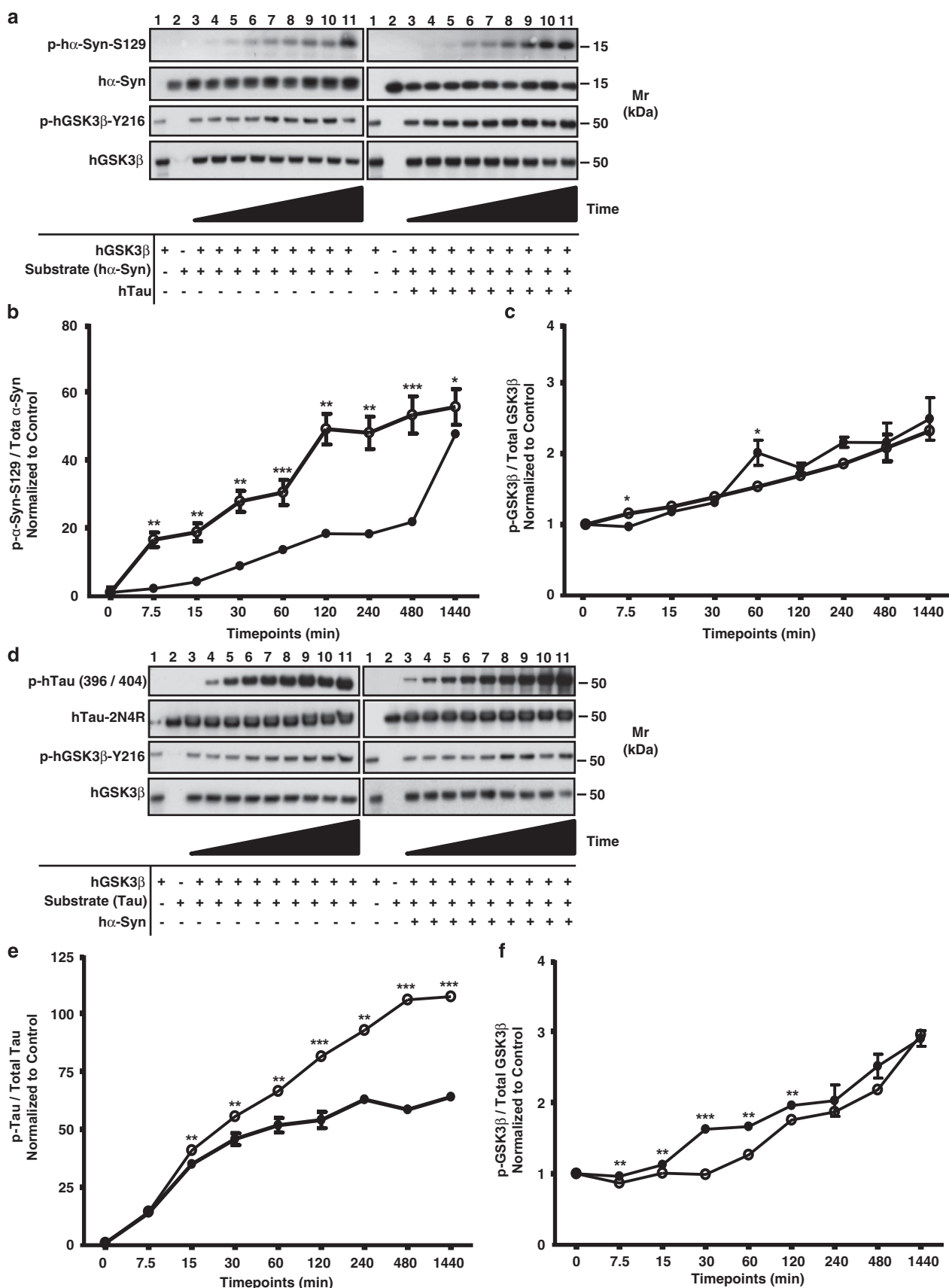
amount of GSK-3 $\beta$  autophosphorylated at Y216, as GSK-3 $\beta$  was equally phosphorylated in the presence or absence of Tau (Figure 6c). Parallel studies were also conducted in equivalent assay conditions to examine whether  $\alpha$ -Syn influenced the formation of p-Tau (Figures 6d–f). Although the presence of  $\alpha$ -Syn increased the overall magnitude of p-Tau levels, the  $t_{1/2}$  of p-Tau formation was unchanged ( $t_{1/2} = 15$  min), regardless of the presence or absence of  $\alpha$ -Syn. (Figures 6d and e). Similar to p-Tau,  $\alpha$ -Syn also failed to affect the conversion of GSK-3 $\beta$  to p-GSK-3 $\beta$ -Y216 (Figure 6f). Together, these data indicate that the presence of  $\alpha$ -Syn or p-Tau differentially affects the phosphorylation of each other, without altering the rate or magnitude of autophosphorylation of GSK-3 $\beta$  at Y216.

## Discussion

The data presented here show the *in vivo* consequences of GSK-3 $\beta$  dysregulation, which is strongly associated with the development of Parkinson-like behavioral and physiological changes in mice in an age-dependent and regional manner. In addition to motor abnormalities, these mice also develop the cardinal features of PD pathology, namely, shrinkage of SN, loss of TH+ neurons, reduced production of DA, and accumulation of  $\alpha$ -Syn, p- $\alpha$ -Syn, and p-Tau in TH+ neurons of SN. Several reports have linked GSK-3 $\beta$  polymorphisms to the genesis of familial and sporadic PD with increased GSK-3 $\beta$  activity and increased p-Tau formation.<sup>53–55</sup> Other studies have provided evidence supporting the direct activation of GSK-3 $\beta$  through physical interactions with mutant forms of LRRK-2, a gene commonly associated with increased risk of developing familial associated PD.<sup>25,26</sup> The aforementioned studies combined with our current results suggest that hyperactivation of GSK-3 $\beta$  may be the primary mechanism by which this protein is linked to PD (Figure 7). Indeed, a growing body of evidence from our laboratory and others define the important roles, kinases, such as GSK-3 $\beta$ , CK2, PLK2 and 3, and GRK1-5 have in the development and pathology of PD through the phosphorylation of  $\alpha$ -Syn and Tau<sup>16,18–24,53–57</sup> (Supplementary Table S3 and associated references).

In response to stressors such as oxidative stress, GSK-3 $\beta$  is converted to its kinase-active form, p-GSK-3 $\beta$ -Y216, resulting in the increased phosphorylation of target substrates such as Tau. In our TG mouse model, there is brain-wide activation of GSK-3 $\beta$  at all ages, because of the overexpression of hGSK-3 $\beta$ -S9A. Yet, accumulation of  $\alpha$ -Syn accompanied by the formation of p- $\alpha$ -Syn and p-Tau is only seen in midbrain neurons of 15-month-old mice. Moreover, even though p-GSK-3 $\beta$ -Y216 levels are increased in the frontal cortex, this region notably lacks elevated  $\alpha$ -Syn or Tau with no formation of the respective phosphorylated forms found. Although the reason for selective spatial formation of phosphorylated  $\alpha$ -Syn and Tau is not clear at this time, we postulate that such

**Figure 6** GSK-3 $\beta$  phosphorylation rate accelerated by dual influence of  $\alpha$ -Syn and Tau. (a–f) Time course experiments. A total of 74.21 ng of hGSK-3 $\beta$  was incubated with substrate (h $\alpha$ -Syn, 1.45  $\mu$ g a–c, or hTau, 4.59  $\mu$ g d–f) in the absence (closed circles) or presence (open circles) of trace levels of either hTau (0.046  $\mu$ g or 100 fM) or h $\alpha$ -Syn (0.015  $\mu$ g or 1 pM). Reactions were conducted for the following times: lanes 1 and 2 = control; lane 3 = 0 min; lane 4 = 7.5 min; lane 5 = 15 min; lane 6 = 30 min; lane 7 = 60 min; lane 8 = 120 min; lane 9 = 240 min; lane 10 = 480 min; lane 11 = 1440 min. Each reaction was analyzed by western blots from three separate and independent studies. p-hTau (Ser396/Ser404), p-h $\alpha$ -Syn-S129, and p-hGSK-3 $\beta$ -Y216 was normalized to total unphosphorylated forms. Comparisons between data were made using Welch's  $t$  test, and significance was measured as \* $P$ <0.05 or \*\* $P$ <0.01 or \*\*\* $P$ <0.001. See also Supplementary Figures S4A and D



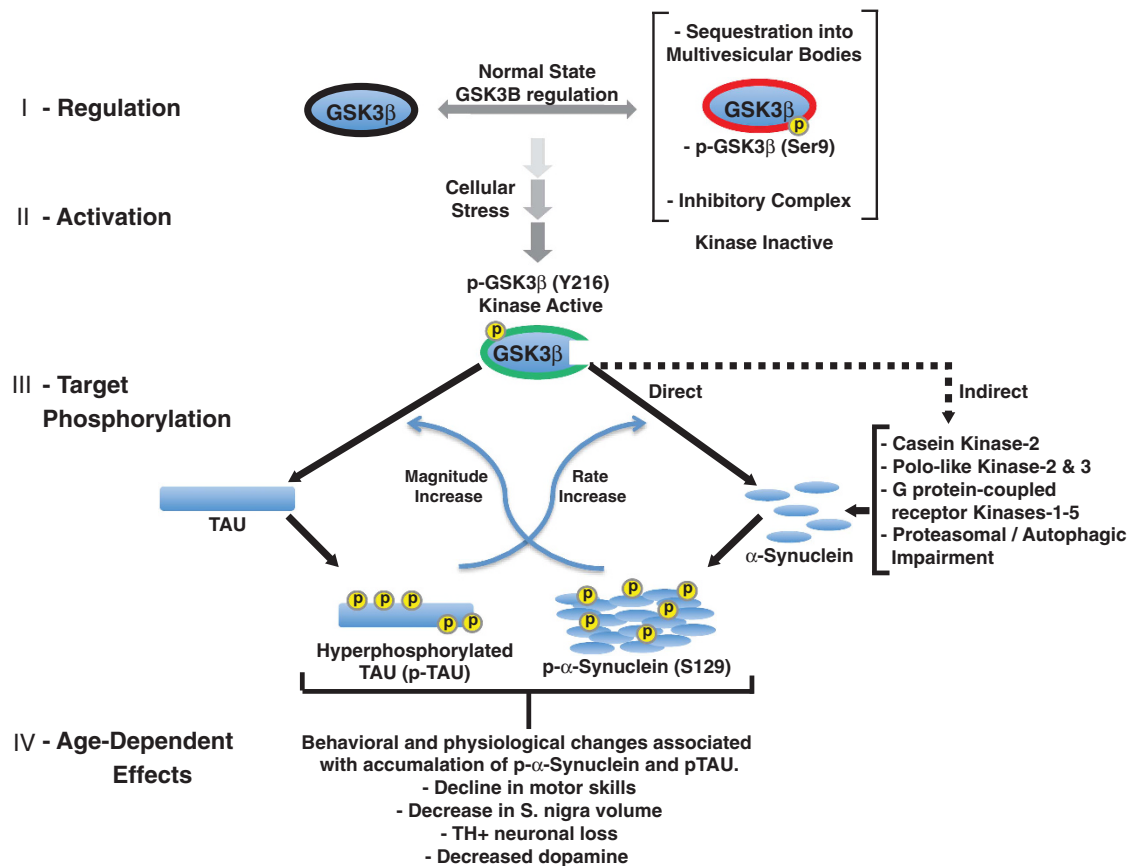


**Figure 7** Model of how GSK3 $\beta$  may contribute to the pathobiology of PD through the dual accumulation of phosphorylated  $\alpha$ -Syn (S129) and Tau (various epitopes). (i) GSK3 $\beta$  is a central regulator of many diverse yet essential cellular signaling networks. GSK3 $\beta$  is therefore highly regulated through various physical interactions and biochemical modifications. (ii) Activation of GSK3 $\beta$  is thought to occur through known and yet-discovered avenues including activation by cellular stresses such as oxidative stress. (iii) Activated GSK3 $\beta$  is known to hyperphosphorylate Tau at a number of sites in both AD and PD. Through the use of *in vitro* kinase assays together with analysis of the hGSK3 $\beta$ -S9A TG mouse model, this study provides evidence that  $\alpha$ -Syn phosphorylation is enhanced via activated GSK3 $\beta$  (p-GSK3 $\beta$ -Y216). Two possible modes of GSK3 $\beta$  mediated effects on  $\alpha$ -Syn phosphorylation are possible. One, directly, with  $\alpha$ -Syn being a substrate for phosphorylation by p-GSK3 $\beta$ -Y216. Two, indirectly, through p-GSK3 $\beta$ -Y216-mediated alterations to cellular signaling pathways leading to the increased expression, activation, or interactions of kinases known to phosphorylate  $\alpha$ -Syn such as casein kinase-2, polo-like kinases-2 and 3, and the G-protein coupled receptor kinases-1-5. Other possible indirect means include p-GSK3 $\beta$ -Y216-mediated reductions in the cells ability to efficiently degrade proteins through the proteasomal and autophagic pathways. In this study,  $\alpha$ -Syn and Tau are also shown to be capable of enhancing the rate or magnitude of phosphorylation of the other by GSK3 $\beta$ . (iv) Pathological and phenotypic changes associated with the phosphorylation and accumulation of Tau and  $\alpha$ -Syn include declines in motor skills, decrease in SN volume, decreased DA, and TH+ neuronal loss.

pathology in midbrain may be due to impairment of the ubiquitin proteasomal and of the autophagic lysosomal pathways together with the unique oxidative environment found in DA-neurons. p-Tau,  $\alpha$ -Syn, and p- $\alpha$ -Syn-S129 are known to decrease activity of proteasomes and lysosomes.<sup>58,59</sup> In addition, GSK-3 $\beta$  can activate mTOR (mammalian target of rapamycin), which is a potent overall inhibitor of autophagy.<sup>60</sup> Regardless of the precise mechanism, the fact remains that TH+ neurons of the midbrain containing high levels of p- $\alpha$ -Syn,  $\alpha$ -Syn, and p-Tau, selectively degenerate, whereas TH-negative neurons of the midbrain, frontal cortex, and striatum remain unaffected. Such conditions of reduced protein turnover may suggest how GSK-3 $\beta$  indirectly influences levels of the phosphorylated proteins without directly participating in their respective phosphorylation.

Indirect activation of GSK-3 $\beta$  through oxidative stress is also supported through studies showing the involvement of reactive astrocytes and microglia as important mediators of GSK-3 $\beta$  regulation.<sup>35,36</sup> Such non-neuronal cells of the CNS

have been shown to be instrumental in orchestrating pathways involved in both repair, and in exacerbating neuronal injury, when oxidative stress is present. Ageing and disease onset may decrease microglial/astrocytes function, with such cells losing the ability to repress GSK-3 $\beta$  activation through decreased Wnt-1 signaling, resulting in the loss of stabilized nuclear  $\beta$ -catenin and subsequent loss of the induction of neural protective  $\beta$ -catenin-specific gene expression programs.<sup>61,62</sup>

The ability of p-GSK-3 $\beta$ -Y216 to phosphorylate  $\alpha$ -Syn on S129 was not previously known. This novel finding is strengthened by our discovery that  $\alpha$ -Syn is phosphorylated by GSK-3 $\beta$  at a single site, S129. In addition to GSK-3 $\beta$ , there are other kinases known to phosphorylate  $\alpha$ -Syn such as GRK1-5, PLK2 and 3, and CK2. The aforementioned kinases, however, do not have the ability to phosphorylate Tau (*Supplementary Figures S4A and D*). *In vitro* assays and cell-based experiments have revealed that CK2, PLK2, and the GRK kinases can readily phosphorylate  $\alpha$ -Syn. Yet no

comprehensive studies exist analyzing the role of aforementioned kinases in targeted phosphorylation of  $\alpha$ -Syn in TG mice overexpressing these individual kinases. Analysis of midbrain tissue from 15-month-old WT and TG mice for detection of differences in expression levels of kinases known to phosphorylate  $\alpha$ -Syn revealed that only CK2 showed elevated expression in TG mice (WT 100% versus TG 151%) (Supplementary Figures S5A and B). However, the unchanged expression levels for the PLK and GRK kinases family members do not negate the possibility that the aforementioned kinases may have increased activation and/or increased physical interactions with  $\alpha$ -Syn independent of their respective expression levels. The activation states and respective expression levels of GRK1-5, PLK2 and 3, and CK2 have, to date, not been analyzed in relevant tissue of the SN from PD patients (see Supplementary Table S3 for detailed comparison of kinases involved in the phosphorylation of  $\alpha$ -Syn). This leaves GSK-3 $\beta$  as the only currently known kinase that can phosphorylate both  $\alpha$ -Syn (*in vitro*) and Tau (*in vivo* and *in vitro*). Although definitive *in vivo* evidence showing that GSK-3 $\beta$  can directly phosphorylate  $\alpha$ -Syn remains unanswered, the ability of GSK-3 $\beta$  to influence both phosphorylation and accumulation of  $\alpha$ -Syn and Tau may provide insight into the cytotoxic role this particular kinase has in the degeneration of TH+ neurons.

Accumulating evidence supports the notion that the formation of p-Tau and the affects of Tau on  $\alpha$ -Syn aggregation may be a common denominator in neurodegenerative synucleopathies and taupathies. In particular, the role of Tau/p-Tau in PD is poorly understood, despite genetic evidence demonstrating linkage of the *MAPT* gene to PD. Several reports in postmortem PD brains have shown the presence of elevated levels of p-Tau. In an extensive study on identifying Tau epitopes that are phosphorylated in postmortem brains from PD, AD, and dementia with Lewy bodies, we have found that the greatest number of phosphorylated sites existed in AD brains. By contrast, in PD brains, of the 20 potential phosphoepitopes analyzed, PD Tau was found to be phosphorylated at 10 of these sites. Our finding that Tau in midbrain of hGSK-3 $\beta$ -S9A mice is phosphorylated at 8 of the 10 sites found in PD, demonstrates 80% overlap with PD. Together, these data suggest that hyperphosphorylation of Tau may potentiate cytotoxic consequences directly and indirectly through its influence on  $\alpha$ -Syn aggregation and phosphorylation in the midbrain of the GSK3- $\beta$ -S9A TG mice.

Our *in vitro* data also provide interesting insight into the manner by which  $\alpha$ -Syn and Tau modulate the phosphorylation of one another without affecting the activity of GSK-3 $\beta$  itself (Figures 5e–h). p- $\alpha$ -Syn formed through the actions of other kinases (CK-2, PLK2 and 3, and GRK1-5) could also contribute to increased Tau phosphorylation and thus contribute to the increased phosphorylation and accumulation of both Tau and  $\alpha$ -Syn. A recent study also showed that in *in vitro* kinase reactions, GSK3- $\beta$ -mediated phosphorylation of Tau was increased in the presence of  $\alpha$ -Syn in a dose-dependent manner.<sup>57</sup> These cumulative findings demonstrate that both  $\alpha$ -Syn and Tau can modulate the toxic production of their phospho-proteins, in a manner that is subtly nuanced (Figure 7).

Future experiments will delineate the exact signaling pathways altered by GSK-3 $\beta$  in the hGSK3- $\beta$ -S9A mouse model, and as such, may provide a more thorough view as to whether phosphorylation of  $\alpha$ -Syn occurs directly or indirectly via p-GSK3- $\beta$ -Y216 and why the occurrence of accumulated p- $\alpha$ -Syn and p-Tau are restricted to the SN. To summarize, these data show that the hGSK3- $\beta$ -S9A PD mouse model developed many of the cardinal features of PD. Given that GSK-3 $\beta$  is highly inducible by oxidative stress, and has now been shown to be capable of phosphorylating two primary proteins that are known to be genetically linked to PD, leading to elevated toxicity, which ultimately culminates in PD, it is likely that GSK-3 $\beta$  will emerge as an important contributor in the genesis of this disease.

## Materials and Methods

**Materials.** With the exception of antibodies against S396/404 and S202 Tau, all antibodies used in this study were obtained from commercial sources, and are described in detail in Supplementary Table S1.

**Animals.** Male and female transgenic mice were obtained from Janssen Research & Development (Breeze, Belgium), and a breeding colony was established at the animal facility at Georgetown University Medical Center. The transgenic mice were generated as described previously<sup>43</sup> and was bred with normal nontransgenic mice with a FVB/NTac background to generate heterozygous mice. All housing, breeding, and procedures were performed according to the NIH Guide for the Care and Use of Experimental Animals and approved by the Georgetown University Animal Care and Use Committee.

**Behavioral analyses.** To evaluate motor behavior, WT and TG mice were tested using a comprehensive battery of behavioral test. The order of tests was randomized and all tests, except gait test, were recorded by video, conducted and scored by an experimenter blinded to the strain. Mice were habituated to the testing room 1 h before tests, and the apparatuses were cleaned with 70% ethanol in between animals to minimize odor cues. All mice were pre-trained prior to conducting tests. The ages of the mice used were: 4–6, 9, 12, and 15 months. See supplementary material and methods for further details.

**Diffusion tensor MRI.** MRI was performed at the Preclinical Imaging Research Laboratory of the Lombardi Cancer Center, Georgetown University on a 7.0 Tesla Bruker (Billerica, MA, USA) horizontal spectrometer/imager with a 20 cm bore equipped with 100 gauss/cm microimaging gradients and run by Paravision 5.0 software (Billerica, MA, USA), as described previously.<sup>63,64</sup> Mice were kept under anesthesia with 1.5% isoflurane and 30% nitrous oxide, positioned in a custom-made stereotaxic animal holder with temperature and respiration control and imaged with a 4 channel-phased array—mouse brain coil. The imaging protocol used was a T2-weighted Turbo RARE (rapid acquisition with rapid enhancement) two-dimensional sequence. Imaging parameters were matrix: 256 × 256 × 256, TR: 3500 ms, TE: 36 ms, number of averages: 4, number of echoes: 1, Rare factor: 8, FOV: 2.5 × 2.5 × 2.5 cm. Volume measurements were performed with the use of Paravision 5.0 software with experimenters blinded to mouse group details by manual tracing of anatomical regions of interest (whole brain and SN) in every image slice and calculating volume based on the slice thickness and inter-slice distance. For the 4-month-old mice, four mice each were used for WT and TG; for the 15-month-old mice, there were four mice for WT and three mice for the TG group. Data obtained from the multiple mice within each group were pooled, and results obtained from TG mice were compared with the WT animals.

**Preparation of lysates and western blot analyses.** Tissues were prepared as previously described.<sup>12,19,20</sup> See supplementary material and methods for further details.

**Immunoblot analysis.** Western blot analyses of mouse tissue homogenates were performed as previously described.<sup>12</sup> See supplementary material and methods for further details.

**Immunohistochemistry.** IHC analysis of mouse brain coronal sections was performed as previously described.<sup>19,65</sup> See supplementary material and methods for further details.

**Immunohistochemistry and stereological counting of SN pars compacta neurons.** Unbiased stereological counts of TH+ and TH – neurons of WT and TG mice was performed as previously described.<sup>66</sup> Briefly, 4% PFA-perfused brains were incubated in a final soak of 30% sucrose, 1× PBS, pH 7.4, followed by serial sectioning at a thickness of 30  $\mu$ m through the SNpc, sampling one in three sections. TH immunohistochemistry (1 : 300, Millipore, Billerica, MA, USA) and Nissl substance neutral red counter staining was performed on individual complete sections (Nissl, Gral Scientific, Victoria, Australia). The total number of DA-neurons in the SNpc was estimated using a fractionator sampling design. Counts were made at regular predetermined intervals ( $x = 140 \mu\text{m}$ ,  $y = 140 \mu\text{m}$ ). Systematic samples of the area occupied by the nuclei were made from a random starting point. An unbiased counting frame of known area (45  $\mu\text{m} \times 35 \mu\text{m}$ ) was superimposed on the image of the tissue sections using stereology software (MBF, Billerica, MA, USA; Stereo Investigator) utilizing a 63× objective lens (Leica, Washington, DC, USA; N.A.1.36). Experimenters were blinded to the treatments of each of the groups.

**In vitro GSK-3 $\beta$  kinase assays.** In vitro kinase assays<sup>67,68</sup> were preformed as previously described with slight modification. Three micromoles of recombinant human  $\alpha$ -Syn ( $\alpha$ -Syn), 1–140 aa (R-peptide, Bogart, GA, USA), or recombinant human Tau-2N4R (hTau-2N4R) (R-peptide), were incubated with 33.0 nM of the following individual kinases; recombinant human GSK-3 $\beta$  (hGSK-3 $\beta$ ) (Promega, Madison, WI, USA), human polo-like kinase-2 (hPLK2) (Carna Biosciences, Natick, MA, USA), casein kinase-2 (hCK2) (Millipore), or human G-protein-coupled receptor kinase-5 (hGRK5) (MBL, Woburn, MA, USA) in 50  $\mu\text{l}$  of kinase buffer (25 mM MOPS, pH 7.2, 12.5 mM  $\beta$ -glycerol-phosphate, 25 mM MgCl<sub>2</sub>, 5 mM EGTA, and 2 mM EDTA) supplemented with 0.2 mM ATP, 50  $\mu\text{M}$  DTT at 25 °C for indicated times. Reactions were terminated with the addition of 100  $\mu\text{l}$  of Laemmli buffer containing  $\beta$ -mercaptoethanol for immunoblot analysis. Mixed kinase reactions including hGSK-3 $\beta$ ,  $\alpha$ -Syn, and hTau-2N4R (the longest human Tau isoform) were at concentrations described in the legend to Figure 4. All reactions were prepared on ice until the start of respective time course.

**DA and metabolite analysis.** DA measurements were conducted by reverse-phase HPLC as described previously.<sup>69</sup> Tissue pellets were dissolved in 1 N NaOH and assayed for protein. Neurochemical concentrations were determined by normalizing samples to protein concentrations. All results were expressed as mean  $\pm$  S.E.M. and statistically analyzed by the Student's *t* test between two groups and analysis of variance among multiple groups. Statistical significance was accepted at the ( $P < 0.05$ ) level.

**Mass spectroscopy–MALDI-TOF.** Mass spectroscopy analysis was conducted on *in vitro* kinase reactions prepared as previously described<sup>70</sup> with the following exceptions: 3.0  $\mu\text{M}$   $\alpha$ -Syn, was incubated with 33.0 nM of hGSK-3 $\beta$ . Samples were de-salted by spin chromatography and analyzed using a 4800 MALDI-TOF-TOF Mass Spectrometer (Applied Biosystems, Carlsbad, CA, USA).

**Statistical analysis.** Results for immunoblots, *in vitro* kinase assays, and behavior analyses are expressed as mean  $\pm$  S.E.M. unless otherwise noted. Significance was determined for behavior test, immunoblots, and kinase assays using un-paired two-tailed Welch's *t*-tests or one-way ANOVA. Statistical significance was accepted at  $P < 0.05$  and is denoted with a single asterisk (\*). Additional statistical distinctions are made at  $P < 0.01$  (\*\*) and  $P < 0.001$  (\*\*\*)�

## Conflict of Interest

The authors declare no conflict of interest.

1. Fearnley JM, Lees AJ. Ageing and Parkinson's disease: substantia nigra regional selectivity. *Brain* 1991; **114**: 2283.
2. Mata IF, Yearout D, Alvarez V, Coto E, de Mena L, Ribacoba R et al. Replication of MAPT and SNCA, but not PARK16-18, as susceptibility genes for parkinson's disease. *Mov Disord* 2011; **26**: 819–823.
3. Edwards TL, Scott WK, Almonte C, Burt A, Powell EH, Beecham GW et al. Genome-wide association study confirms SNPs in SNCA and the MAPT region as common risk factors for Parkinson disease. *Ann Hum Genet* 2010; **74**: 97–109.
4. Simón-Sánchez J, Schulte C, Bras JM, Sharma M, Gibbs JR, Berg D et al. Genome-wide association study reveals genetic risk underlying Parkinson's disease. *Nat Genet* 2009; **41**: 1308–1312.
5. Yasuda T, Nakata Y, Mochizuki H.  $\alpha$ -Synuclein and neuronal cell death. *Mol Neurobiol* 2013; **47**: 466–483.
6. Houlden H, Singleton AB. The genetics and neuropathology of Parkinson's disease. *Acta Neuropathol* 2012; **124**: 325–338.
7. Fujiwara H, Hasegawa M, Dohmae N, Kawashima A, Masliah E, Goldberg MS et al. alpha-Synuclein is phosphorylated in synucleinopathy lesions. *Nat. Cell Biol* 2002; **4**: 160–164.
8. Anderson JP, Walker DE, Goldstein JM, de Laat R, Banducci K, Caccavello RJ et al. Phosphorylation of Ser-129 is the dominant pathological modification of alpha-synuclein in familial and sporadic Lewy body disease. *J Biol Chem* 2006; **281**: 29739–29752.
9. Chen L, Feany MB. Alpha-synuclein phosphorylation controls neurotoxicity and inclusion formation in a Drosophila model of Parkinson disease. *Nat Neurosci* 2005; **8**: 657–663.
10. Oueslati A, Fournier M, Lashuel HA. Role of post-translational modifications in modulating the structure, function and toxicity of  $\alpha$ -synuclein: implications for Parkinson's disease pathogenesis and therapies. *Prog Brain Res* 2010; **183**: 115–145.
11. Ishizawa T, Mattila P, Davies P, Wang D, Dickson DW. Colocalization of tau and alpha-synuclein epitopes in Lewy bodies. *J Neuropathol Exp Neurol* 2003; **62**: 389–397.
12. Duka V, Lee JH, Credle J, Wills J, Oaks A, Smolinsky C et al. Identification of the sites of tau hyperphosphorylation and activation of tau kinases in synucleinopathies and Alzheimer's diseases. *PLoS One* 2013; **8**: e75025.
13. Wills J, Jones J, Haggerty T, Duka V, Joyce JN, Sidhu A. Elevated taupathy and alpha-synuclein pathology in postmortem Parkinson's disease brains with and without dementia. *Exp Neurol* 2010; **225**: 210–218.
14. Colom-Cadenas M, Gelpi E, Charif S, Belbin O, Blesa R, Martí MJ et al. Confluence of  $\alpha$ -Synuclein, Tau, and  $\beta$ -amyloid pathologies in dementia with Lewy bodies. *J Neuropathol Exp Neurol* 2013; **72**: 1203–1212.
15. Muntaué G, Dalfó E, Martínez A, Ferrer I. Phosphorylation of tau and alpha-synuclein in synaptic-enriched fractions of the frontal cortex in Alzheimer's disease, and in Parkinson's disease and related alpha-synucleinopathies. *Neuroscience* 2008; **152**: 913–923.
16. Duka T, Duka V, Joyce JN, Sidhu A. Alpha-Synuclein contributes to GSK-3beta-catalyzed Tau phosphorylation in Parkinson's disease models. *FASEB J* 2009; **23**: 2820–2830.
17. Wills J, Credle J, Oaks AW, Duka V, Lee JH, Jones J et al. Paraquat, but not maneb, induces synucleinopathy and taupathy in striata of mice through inhibition of proteasomal and autophagic pathways. *Plos One* 2012; **7**: e30745.
18. Qureshi HY, Paudel HK. Parkinsonian neurotoxin 1-methyl-4-phenyl-1,2,3,6-tetrahydropyridine [MPTP] and alpha-synuclein mutations promote Tau protein phosphorylation at Ser262 and destabilize microtubule cytoskeleton in vitro. *J Biol Chem* 2011; **286**: 5055–5068.
19. Wills J, Credle J, Haggerty T, Lee JH, Oaks AW, Sidhu A. Taupathic changes in the striatum of A53T  $\alpha$ -synuclein mutant mouse model of Parkinson's disease. *Plos One* 2011; **6**: e17953.
20. Haggerty T, Credle J, Rodriguez O, Wills J, Oaks AW, Masliah E et al. Hyperphosphorylated Tau in an  $\alpha$ -synuclein overexpressing transgenic model of Parkinson's disease. *Eur J Neurosci* 2011; **33**: 1598–1610.
21. Compta Y, Parkkinen L, Kempster P, Selikhova M, Lashley T, Holton JL et al. The significance of  $\alpha$ -synuclein, amyloid- $\beta$  and tau pathologies in Parkinson's disease progression and related dementia. *Neurodegener Dis* 2014; **13**: 154–156.
22. Kang JH, Irwin DJ, Chen-Plotkin AS, Siderowf A, Caspell C, Coffey CS et al. Parkinson's Progression Markers Initiative Association of cerebrospinal fluid  $\beta$ -amyloid 1-42, T-tau, P-tau181, and  $\alpha$ -synuclein levels with clinical features of drug-naïve patients with early Parkinson disease. *JAMA Neurol* 2013; **70**: 1277–1287.
23. Irwin DJ, Lee VM, Trojanowski JQ. Parkinson's disease dementia: convergence of  $\alpha$ -synuclein, tau and amyloid- $\beta$  pathologies. *Nat Rev Neurosci* 2013; Sep; **14**: 626–636.
24. Ciaccioli G, Martins A, Rodrigues C, Vieira H, Calado P. A powerful yeast model to investigate the synergistic interaction of  $\alpha$ -synuclein and tau in neurodegeneration. *PLoS One* 2013; **8**: e55848.
25. Lin CH, Tsai PI, Wu RM, Chien CT. LRRK2 G2019S mutation induces dendrite degeneration through mislocalization and phosphorylation of tau by recruiting autoactivated GSK3beta. *J Neurosci* 2010; **30**: 13138–13149.
26. Kawakami F, Shimada N, Ohta E, Kagiyama G, Kawashima R, Maekawa T et al. Leucine-rich repeat kinase 2 regulates tau phosphorylation through direct activation of glycogen synthase kinase-3 $\beta$ . *FEBS J* 2014; **281**: 3–13.
27. Hernandez F, Lucas JJ, Avila J. GSK3 and tau: two convergence points in Alzheimer's disease. *J Alzheimers Dis* 2013; **33**: S141–S144.
28. Hanger DP, Noble W. Functional implications of glycogen synthase kinase-3-mediated tau phosphorylation. *Int J Alzheimers Dis* 2011; 352805.
29. Cole A, Frame S, Cohen P. Further evidence that the tyrosine phosphorylation of glycogen synthase kinase-3 (GSK3) in mammalian cells is an autophasphorylation event. *Biochem J* 2004; **377**: 249–255.
30. Lochhead PA, Kintrie R, Sibbet G, Rawjee T, Morrice N, Cleghon V. A chaperone-dependent GSK3beta transitional intermediate mediates activation-loop autophasphorylation. *Mol Cell* 2006; **24**: 627–633.

31. Ilouz R, Pietrovski S, Eisenstein M, Eldar-Finkelman H. New insights into the autoinhibition mechanism of glycogen synthase kinase-3beta. *J Mol Biol* 2008; **383**: 999–1007.
32. Ikeda S, Kishida S, Yamamoto H, Murai H, Koyama S, Kikuchi A. Axin, a negative regulator of the Wnt signaling pathway, forms a complex with GSK-3beta and beta-catenin and promotes GSK-3beta-dependent phosphorylation of beta-catenin. *EMBO J* 1998; **17**: 1371–1384.
33. Yost C, Farr GH 3rd, Pierce SB, Ferkey DM, Chen MM, Kimelman D. GBP an inhibitor of GSK-3, is implicated in Xenopus development and oncogenesis. *Cell* 1998; **93**: 1031–1041.
34. Taelman VF, Dobrowski R, Plouhinec JL, Fuentelba LC, Vorwald PP, Gumper I et al. Wnt signaling requires sequestration of glycogen synthase kinase 3 inside multivesicular endosomes. *Cell* 2010; **143**: 1136–1148.
35. L'Episcopo F, Tirolo C, Testa N, Caniglia S, Morale MC, Cossetti C et al. Reactive astrocytes and Wnt/ $\beta$ -catenin signaling link nigrostriatal injury to repair in 1-methyl-4-phenyl-1,2,3,6-tetrahydropyridine model of Parkinson's disease. *Neurobiol Dis* 2011; **41**: 508–527.
36. L'Episcopo F, Tirolo C, Testa N, Caniglia S, Morale MC, Serapide MF et al. Wnt/ $\beta$ -catenin signaling is required to rescue midbrain dopaminergic progenitors and promote neurorepair in ageing mouse model of Parkinson's disease. *Stem Cells* 2014; **32**: 2147–2163.
37. Gómez-Sintes R, Hernández F, Bortolozzi A, Artigas F, Avila J, Zaratin P et al. Neuronal apoptosis and reversible motor deficit in dominant-negative GSK-3 conditional transgenic mice. *EMBO J* 2007; **26**: 2743–2754.
38. Lucas JJ, Hernández F, Gómez-Ramos P, Morán MA, Hen R, Avila J. Decreased nuclear beta-catenin, tau hyperphosphorylation and neurodegeneration in GSK-3beta conditional transgenic mice. *EMBO J* 2001; **20**: 27–39.
39. Gordon JW, Chesa PG, Nishimura H, Rettig WJ, Maccari JE, Endo T et al. Regulation of Thy-1 gene expression in transgenic mice. *Cell* 1987; **50**: 445–452.
40. Mayford M, Wang J, Kandel ER, O'Dell TJ. CaMKII regulates the frequency-response function of hippocampal synapses for the production of both LTD and LTP. *Cell* 1995; **81**: 891–904.
41. Petit-Paitel A, Brau F, Cazareth J, Chabry J. Involvement of cytosolic and mitochondrial GSK-3beta in mitochondrial dysfunction and neuronal cell death of MPTP/MPP+ treated neurons. *PLoS One* 2009; **4**: e5491.
42. Hongo H, Kihara T, Kume T, Izumi Y, Niidome T, Sugimoto H et al. Glycogen synthase kinase-3 $\beta$  activation mediates rotenone-induced cytotoxicity with the involvement of microtubule destabilization. *Biochem Biophys Res Commun* 2012; **426**: 94–99.
43. Spittaels K, Van den Houte C, Van Dorpe J, Terwel D, Vandezande K, Lasrado R et al. Neonatal neuronal overexpression of glycogen synthase kinase-3 beta reduces brain size in transgenic mice. *Neuroscience* 2002; **113**: 797–808.
44. Chesselet MF, Richter F. Modelling of Parkinson's disease in mice. *Lancet Neurol* 2011; **10**: 1108–1118.
45. Cochrane CJ, Ebmeier KP. Diffusion tensor imaging in parkinsonian syndromes: a systematic review and meta-analysis. *Neurology* 2013; **80**: 857–864.
46. Ziegler DA, Wonderlick JS, Ashourian P, Hansen LA, Young JC, Murphy AJ et al. Substantia nigra volume loss before basal forebrain degeneration in early Parkinson disease. *JAMA Neurol* 2013; **70**: 241–247.
47. Lundblad M, Decressac M, Mattsson B, Björklund A. Impaired neurotransmission caused by overexpression of  $\alpha$ -synuclein in nigral dopamine neurons. *Proc Natl Acad Sci U S A* 2012; **109**: 3213–3219.
48. Bernheimer H, Birkmayer W, Hornykiewicz O, Jellinger K, Seitelberger F. Brain dopamine and the syndromes of Parkinson and Huntington. Clinical, morphological and neurochemical correlations. *J Neurol Sci* 1973; **20**: 415–455.
49. Riederer P, Wuketich S. Time course of nigrostriatal degeneration in parkinson's disease. A detailed study of influential factors in human brain amine analysis. *J Neural Transm* 1976; **38**: 277–301.
50. Zigmund MJ, Abercrombie ED, Berger TW, Grace AA, Stricker EM. Compensations after lesions of central dopaminergic neurons: some clinical and basic implications. *Trends Neurosci* 1993; **13**: 290–296.
51. Hornykiewicz O. Parkinson's disease and the adaptive capacity of the nigrostriatal dopamine system: possible neurochemical mechanisms. *Adv Neurol* 1990; **60**: 140–147.
52. Martinez A, Alonso M, Castro A, Pérez C, Moreno FJ. First non-ATP competitive glycogen synthase kinase 3 beta (GSK-3beta) inhibitors: thiadiazolidinones (TDZD) as potential drugs for the treatment of Alzheimer's disease. *J Med Chem* 2002; **45**: 1292–1299.
53. Kalinderi K, Fidani L, Katsarou Z, Clarimón J, Bostantjopoulou S, Kotsis A. GSK3 $\beta$  polymorphisms, MAPT H1 haplotype and Parkinson's disease in a Greek cohort. *Neurobiol Aging* 2011; **32**: 546.e1–5.
54. Wider C, Vilariño-Güell C, Heckman MG, Jasinska-Myga B, Ortolaza-Soto AI, Diehl NN et al. SNCA, MAPT, and GSK3B in Parkinson disease: a gene-gene interaction study. *Eur J Neurol* 2011; **18**: 876–881.
55. Kwok JB, Hallupp M, Loy CT, Chan DK, Woo J, Mellick GD et al. GSK3B polymorphisms alter transcription and splicing in Parkinson's disease. *Ann Neurol* 2005; **58**: 829–839.
56. Chen G, Bower KA, Ma C, Fang S, Thiele CJ, Luo J. Glycogen synthase kinase 3beta (beta) mediates 6-hydroxydopamine-induced neuronal death. *FASEB J* 2004; **18**: 1162–1164.
57. Kawakami F, Suzuki M, Shimada N, Kaguya G, Ohta E, Tamura K et al. Stimulatory effect of  $\alpha$ -synuclein on the tau-phosphorylation by GSK-3 $\beta$ . *FEBS J* 2011; **278**: 4895–4904.
58. Chau KY, Ching HL, Schapira AH, Cooper JM. Relationship between alpha synuclein phosphorylation, proteasomal inhibition and cell death: relevance to Parkinson's disease pathogenesis. *J Neurochem* 2009; **110**: 1005–1013.
59. Wakamatsu M, Ishii A, Ukai Y, Sakagami J, Iwata S, Ono M et al. Accumulation of phosphorylated alpha-synuclein in dopaminergic neurons of transgenic mice that express human alpha-synuclein. *J Neurosci Res* 2007; **85**: 1819–1825.
60. Hung CM, Garcia-Haro L, Sparks CA, Guerrieri DA. mTOR-dependent cell survival mechanisms. *Cold Spring Harb Perspect Biol* 2012; **4**: pii: a008771.
61. L'Episcopo F, Serapide MF, Tirolo C, Testa N, Caniglia S, Morale MC et al. A Wnt1 regulated Frizzled-1/ $\beta$ -Catenin signaling pathway as a candidate regulatory circuit controlling mesencephalic dopaminergic neuron-astrocyte crosstalk: Therapeutic relevance for neuron survival and neuroprotection. *Mol Neurodegener* 2011; **6**: 49.
62. Marchetti B, L'Episcopo F, Morale MC, Tirolo C, Testa N, Caniglia S et al. Uncovering novel actors in astrocyte-neuron crosstalk in Parkinson's disease: the Wnt/ $\beta$ -catenin signaling cascade as the common final pathway for neuroprotection and self-repair. *Eur J Neurosci* 2013; **37**: 1550–1563.
63. Fricke ST, Rodriguez O, Vanmeter J, Dettin LE, Casimiro M, Chien CD et al. In Vivo Magnetic Resonance Volumetric and Spectroscopic Analysis of Mouse Prostate Cancer Models. *Prostate* 2006; **66**: 708–717.
64. Sirajuddin P, Das S, Ringer L, Rodriguez OC, Sivakumar A, Lee YC et al. Quantifying the CDK inhibitor VMY-1-103's activity and tissue levels in an *in vivo* tumor model by LC-MS/MS and by MRI. *Cell Cycle* 2012; **11**: 3801–3809.
65. Oaks AW, Frankurt M, Finkelstein DI, Sidhu A. Age-dependent effects of A53T alpha-synuclein on behavior and dopaminergic function. *PLoS One* 2013; **8**: e60378.
66. Finkelstein DI, Stanić D, Parish CL, Drago J, Horne MK. Quantified assessment of terminal density and innervation. *Curr Protoc Neurosci* 2004 Chapter 1:Unit 1.13.
67. Sperber BR, Leight S, Goedert M, Lee VM. Glycogen synthase kinase-3 beta phosphorylates tau protein at multiple sites in intact cells. *Neurosci Lett* 1995; **197**: 149–153.
68. Rodriguez-Martín T, Cuchillo-Ibáñez I, Noble W, Nyenga F, Anderton BH, Hanger DP. Tau phosphorylation affects its axonal transport and degradation. *Neurobiol Aging* 2013; **34**: 2146–2157.
69. Gil-Loyzaga P, Parés-Herbute N. HPLC detection of dopamine and noradrenaline in the cochlea of adult and developing rats. *Brain Res Dev Brain Res* 1998; **48**: 157–160.
70. Paleologou KE, Schmid AW, Rospigliosi CC, Kim HY, Lamberto GR, Fredenburg RA et al. Phosphorylation at Ser-129 but not the phosphomimics S129E/D inhibits the fibrillation of alpha-synuclein. *J Biol Chem* 2008; **283**: 16895–16905.

Supplementary Information accompanies this paper on Cell Death and Differentiation website (<http://www.nature.com/cdd>)